

Northumbria Research Link

Citation: Castley, Jack, Azimov, Ulugbek, Combrinck, Madeleine and Xing, Lu (2022) Modeling and optimization of combined cooling, heating and power systems with integrated biogas upgrading. Applied Thermal Engineering, 210. p. 118329. ISSN 1359-4311

Published by: Elsevier

URL: <https://doi.org/10.1016/j.applthermaleng.2022.118329>
<<https://doi.org/10.1016/j.applthermaleng.2022.118329>>

This version was downloaded from Northumbria Research Link:
<https://nrl.northumbria.ac.uk/id/eprint/48638/>

Northumbria University has developed Northumbria Research Link (NRL) to enable users to access the University's research output. Copyright © and moral rights for items on NRL are retained by the individual author(s) and/or other copyright owners. Single copies of full items can be reproduced, displayed or performed, and given to third parties in any format or medium for personal research or study, educational, or not-for-profit purposes without prior permission or charge, provided the authors, title and full bibliographic details are given, as well as a hyperlink and/or URL to the original metadata page. The content must not be changed in any way. Full items must not be sold commercially in any format or medium without formal permission of the copyright holder. The full policy is available online: <http://nrl.northumbria.ac.uk/policies.html>

This document may differ from the final, published version of the research and has been made available online in accordance with publisher policies. To read and/or cite from the published version of the research, please visit the publisher's website (a subscription may be required.)

Modeling and optimization of combined cooling, heating and power systems with
integrated biogas upgrading

Jack Castley, Ulugbek Azimov, Madeleine Combrinck, Lu Xing*

Mechanical and Construction Engineering, Northumbria University, Newcastle upon
Tyne, NE1 8ST, United Kingdom

*Corresponding author:

Lu Xing, lu.xing@northumbria.ac.uk;

Abstract

This paper proposes an analysis for cattle manure-fed anaerobic digestion reactor (ADR), with biogas upgrading technologies, to be integrated into a CCHP system. The aim is to substantiate whether such a system will present economic, environmental, and energy-related benefits over conventional CCHP systems. Eight CCHP configurations have been modeled and optimized. The proposed CCHP systems are applied to an office building, for quantifying and analyzing the system performance for satisfying energy loads within the European building sector in a heating-dominated climate. The CCHP system with an integrated ADR, with a biogas boiler, deploying the electric load operational strategy yields the best results. This system presents an overall performance score of 151.1%, after achieving the best carbon emissions reduction ratio of 93.7%, and the best primary energy saving ratio of 32.0%.

Keywords: Combined cooling heating and power; Anaerobic digestion reactor; System optimization, Biogas, Biomethane

Nomenclature

| | |
|----------------|--|
| ADR | Anaerobic Digestion Reactor |
| ADR-CCHP (FEL) | Combined cooling, heating and power with anaerobic digestion reactor following the electric load |
| ADR-CCHP (FTL) | Combined cooling, heating and power with anaerobic digestion reactor following the thermal load |
| AEC | Annual Energy Costs |
| AEQC | Annual Equipment Capital Costs |
| AI | Artificial Intelligence |
| ATC | Annual Total Costs |
| ATCS | Annual Total Cost Savings |
| ATCSR | Annual Total Cost Savings Ratio |
| BGB | Biogas Compatible Gas |
| CCHP | Combined cooling, heating, and power |
| CE | Carbon Emissions |
| CER | Carbon Emissions Reduction |
| CERR | Carbon Emissions Reduction Ratio |
| CHP | Combined Heat and Power |
| CCHP (FEL) | Combined cooling, heating and power following the electric load |
| CCHP (FTL) | Combined cooling, heating and power following the thermal load |
| COP | Coefficient of Performance |
| CSS | Conventionally Separated System |
| FEL | Following the Electric Load |
| FITs/FIPs | Feed in Tariffs/Premiums |
| FTL | Following the Thermal Load |
| GA | Genetic Algorithm |
| HST | Heat Storage Tank |
| ICE | Internal Combustion Engine |
| LEED | Leadership in Energy and Environmental Design |
| NGB | Natural Gas Boiler |
| OMC | Annual Operation and Maintenance Costs |
| OPI | Overall Performance Index |
| PEC | Primary Energy Consumption |
| | Primary Energy Savings Ratio |
| PGU | Power Generation Unit |
| PSA | Pressure Swing Absorption |
| PSA-CCHP (FEL) | Combined cooling, heating and power with anaerobic digestion reactor and pressure swing absorption following the electric load |
| PSA-CCHP (FTL) | Combined cooling, heating and power with anaerobic digestion reactor and pressure swing absorption following the electric load |
| PSOA | particle swarm optimization algorithm |
| PWS | pressurized water scrubbing |

| | |
|----------------|--|
| PWS-CCHP (FEL) | Combined cooling, heating and power with anaerobic digestion reactor and pressurized water scrubbing following the electric load |
| PWS-CCHP (FTL) | Combined cooling, heating and power with anaerobic digestion reactor and pressurized water scrubbing following the thermal load |
| R | Capital Recovery Factor |
| UF | Utilization Factor |
| VOCs | Volatile Organic Compounds |
| WHR | Waste Heat Recovery Unit |

1. Introduction

Building energy use that is required for space heating, domestic hot water, space cooling and electricity accounts for over 40% of total primary energy consumption in the United States and Europe [1-2]. To meet this demand, most energy is generated using inefficient conventional power plants which usually use carbon-rich fossil fuels. This causes the increase of greenhouse gas emissions, impacting the environment and leading to global warming. The International Energy Agency declared that of the 1.0°C increase of global average annual surface temperatures, coal combustion is responsible for over 0.3°C increase [3].

Combined cooling, heating, and power (CCHP) systems use distributed energy and focus on cascade energy utilization. It is an energy-efficient technology which provides alternative energy solutions. Instead of releasing waste heat from the power generation unit (PGU) of the system into the atmosphere, the heat is harnessed to deliver building heating and cooling. The CCHP system's energy efficiency can reach up to 80% [4].

Buildings require different energy loads due to variable determinate factors such as architectural design, local climate, and energy prices. The complexity of system structure, operational strategy, and the variation of the building loads all set strict requirements for the building energy system design, which is critical for ensuring the building energy efficiency.

Extensive research has been conducted on the optimization of system performance with considerations of variables such as equipment selection, integration, and capacities [4-5] and operational strategies [6-8]. Research showed that biomass utilization is considered in the CCHP system to offer advantages in flexibility, conversion efficiency and commercial

possibility [9-13]. The forementioned research works share the interest of improving at least one of the following parameters: annual total cost savings (ATCS), carbon emissions reduction (CER), and primary energy consumption (PEC). The optimization of these parameters has been conducted in a variety of ways over the years, using methods such as linear programming [14-15], Newtonian methods [16-17], sequential quadratic programming [18-19], yet the most elected methodologies utilize artificial intelligence (AI) programming algorithms, such as the genetic algorithm (GA) [6,11,20] and particle swarm optimization algorithm (PSOA). Wang et al. conducted analysis comparing the energy flows of a Conventionally Separated System (CSS) with a redundant CCHP system [21]. The system was optimized using PSOA and four decision variables: PGU capacity, heat storage tank (HST) capacity, PGU on-off coefficient, the electric cooling-to-cool load ratio. Using the case study of a CCHP system with a HST and hybrid cooling system, the improvement of ATC, PEC and CER was presented to ascertain the feasibility and validity of the optimization method. The annual savings ratios of the optimized CCHP in comparison to the CSS were 12.2%, 11.2%, and 25.9% regarding PEC, ATC, and CER, respectively. Tichi et al. [22] also used PSOA to produce an optimal configuration of combined heat and power (CHP) and CCHP systems. The PSOA was specifically used to minimize the cost function for owning and operating various CHP and CCHP systems in an industrial dairy unit. It was effectively concluded that the current energy price policies hinder the installation of CHP and CCHP systems and identified that policies which provide infrastructure for selling electricity to the grid, as well as eliminating subsidies, are major prerequisites for the successful widespread utilization of cogeneration and trigeneration systems.

Despite the rigorous ongoing studies carried out over CCHP field, there are still areas which could be addressed to improve the energy production and utilization in CCHP systems. One specific area is the consideration and analysis of the potential for a cattle manure fed anaerobic digestion reactor (ADR) in tandem with biogas upgrading technologies to be optimally integrated into a CCHP system to present economical, environmental, and energy-related benefits over typical energy systems, and moreover, over conventional gas-fed CCHP systems [23, 24].

The application and integration of ADR in CCHP systems will help to reduce the direct use of manure and neutralize the environmental impact of cattle manure decomposition such as produced high level of CHG emissions, odor, and contamination of local water reservoirs. For example, lack of manure treatment in the UK results in 28% of all ammonia emissions [25]. Manure and slurry contribute about 50% of anthropogenic UK's methane emissions [25]. With methane having 21 times the global warming potential of carbon dioxide, this is critically detrimental to the environment. In addition, the by-product of anaerobically digested cattle manure (digestate) offers itself as a nutrient rich, more environmentally friendly, and almost odorless fertilizer which can either be used directly by the farmer or sold – providing an additional source of income. Furthermore, biogas produced from cattle manure not only directly reduces carbon emissions by replacing fossil fuels, additionally, it is a carbon-neutral fuel source, since it adds no additional carbon into the atmosphere. The only carbon expelled during its combustion was already in the Earth's atmosphere and comes from the plant matter eaten by the cattle. Using biogas upgrading/cleaning technologies such as water/amine scrubbers [26] or membrane separators [27], the harmful and toxic compounds (H₂S, Si, Volatile Organic Compounds (VOCs), siloxanes, CO, and

NH₃) and the biogas of carbon dioxide can be removed creating an end-product of up to 99% biomethane (CH₄). Biomethane is sufficiently clean, so that traditional boilers and PGUs can utilize it as a fuel source. Moreover, it can be injected directly into the national gas grid where it can create an additional revenue stream in the way of Feed in Tariffs/Premiums (FITs/FIPs).

This paper aims to model potential configurations of a CCHP system integrated with an ADR harnessing a cattle manure feedstock and biogas upgrading plant. Once potential configurations of the model are identified, after producing and utilizing a Particle Swarm Optimization Algorithm (PSOA) within the Matrix Laboratories (MATLAB) environment, they have been applied to the case study of a commercial building's energy loads in a selected location (Krakow, Poland). The optimum design configuration with respect to Annual Total Cost Savings (ATCS), Carbon Emission Reduction (CER), and Primary Energy Consumption (PEC) have been derived. Comparisons between these optimized configurations and typical energy systems, as well as conventional CCHP systems, have been made and, as a result, firmly substantiated whether such a system can be a feasible and beneficial technology used to satisfy energy loads within the European building sector. This study has developed a numerical approach where, a novel PSOA has been derived, which will have the capabilities of optimizing such CCHP configurations with respect to any given building's heating, cooling, and electricity loads, considering ATCS, CER and PEC. Parameters such as unit costs, equipment costs, and equipment efficiencies can be used for any appropriate adjustments (to the end-user's discretion) and the program. The optimized CCHP system's performance has been compared against that of a Conventionally Separated System (CSS), which might typically be found as the source of

energy production for the building(s) under evaluation.

2. Methodology

In this work, eight (8) CCHP configurations have been modelled (Table 1). The performance of these systems was compared against the performance of a conventional separated system (CSS).

Table 1 – System description of the configurations modelled

| Number | System Description | Abbreviation |
|-----------------|--|----------------|
| Reference | Conventional Separated System | CSS |
| Configuration 1 | Combined cooling, heating and power following the electric load | CCHP (FEL) |
| Configuration 2 | Combined cooling, heating and power following the thermal load | CCHP (FTL) |
| Configuration 3 | Combined cooling, heating and power with anaerobic digestion reactor following the electric load | ADR-CCHP (FEL) |
| Configuration 4 | Combined cooling, heating and power with anaerobic digestion reactor following the thermal load | ADR-CCHP (FTL) |
| Configuration 5 | Combined cooling, heating and power with anaerobic digestion reactor and pressurized water scrubbing following the electric load | PWS-CCHP (FEL) |
| Configuration 6 | Combined cooling, heating and power with anaerobic digestion reactor and pressurized water scrubbing following the thermal load | PWS-CCHP (FTL) |
| Configuration 7 | Combined cooling, heating and power with anaerobic digestion reactor and pressure swing absorption following the electric load | PSA-CCHP (FEL) |
| Configuration 8 | Combined cooling, heating and power with anaerobic digestion reactor and pressure swing absorption following the electric load | PSA-CCHP (FTL) |

2.1. Conventionally Separated System

The reference system used as a benchmark for comparison with the CCHP systems

modelled and optimized is the conventionally separated system (CSS) shown in Fig. 1.

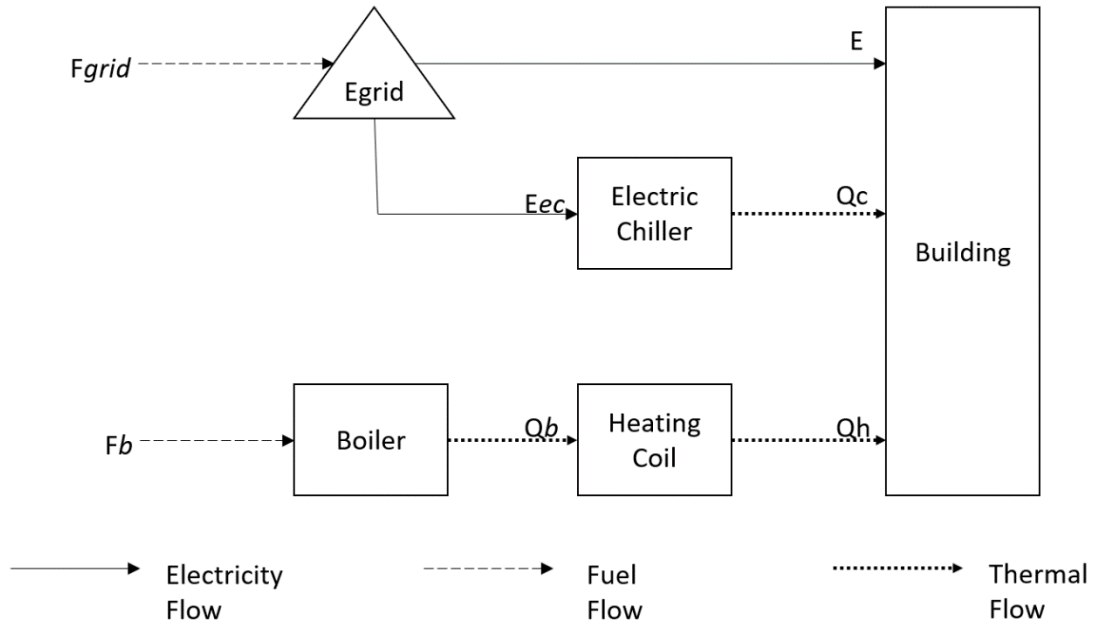


Fig. 1. Energy Flow Diagram of a CSS system

In a CSS, the entirety of the building's electricity load (E) is satisfied by electricity bought from the grid (E_{grid}). The cooling load (Q_c) is met via an electric chiller which is fueled by electricity also bought from the grid (E_{ec}). Finally, the heating load (Q_h) is met by a natural gas boiler (Q_b) which is distributed through the building by means of heating coils. The mathematical model for this system is described by Equations 1 – 7.

The cooling output to the electric chiller, Q_{ec} (kWh) is equal to the cooling load (Q_c):

$$Q_{ec} = Q_c \quad (1)$$

The electrical consumption of the electric chiller, E_{ec} (kWh), is a function of the cooling output and the Coefficient of Performance (COP) of the electric chiller (COP_{ec}):

$$E_{ec} = \frac{Q_{ec}}{COP_{ec}} \quad (2)$$

The electrical balance of the CSS (kWh) summed with the building's electricity load (E) is

equal to the electricity bought from the grid (E_{grid}):

$$E_{ec} + E = E_{grid} \quad (3)$$

Thermal energy output of the natural gas boiler, Q_b (kWh) is equal to the heating load (Q_h):

$$Q_b = Q_h \quad (4)$$

The fuel consumption of the natural gas boiler, F_b (kWh) is a function of the heating load, the boiler efficiency (η_b) and the building heat exchanger efficiency (η_{he}):

$$F_b = \frac{Q_h}{(\eta_b)(\eta_{he})} \quad (5)$$

The fuel consumption of the national grid to power the CSS, F_{grid} (kWh) is described by:

$$F_{grid} = \frac{E_{grid}}{(\eta_{e_css})(\eta_{grid})} \quad (6)$$

where η_{e_css} is the electrical efficiency and η_{grid} is the grid transmission efficiency.

The Primary Energy Consumption (PEC) of the CSS, PEC_{css} (kWh) is calculated as

$$PEC_{css} = \sum F_{grid} + \sum F_b \quad (7)$$

2.2. CCHP with integrated biofuel technologies

Schematics of the eight configurations tested in this study is shown in Figure 2. A conventional system, both for following the electrical load, CCHP (FEL), and the thermal load, CCHP (FTL), is shown in Figure 2a. In Figure 2b an anaerobic digester is added to the system to represent the configurations denoted as ADR-CCHP (FEL) and ADR-CCHP (FTL). The configurations PWS-CCHP (FEL), PWS-CCHP (FTL), PSA-CCHP (FEL) and PSA-CCHP (FTL) are represented in Figure 2c.

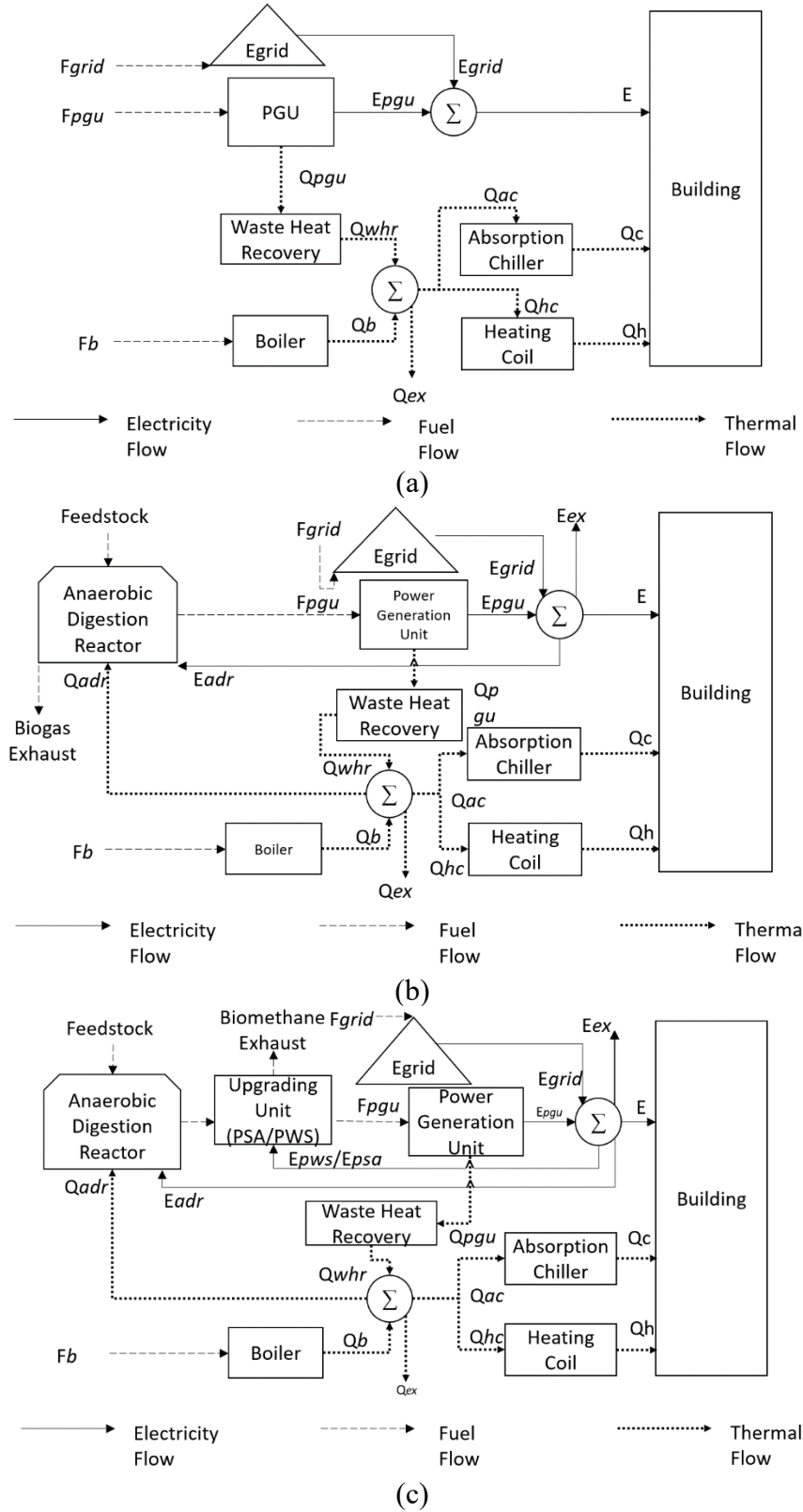


Fig. 2: Energy Flow Diagram of a CCHP system (a) conventional system (b) CCHP

system with an integrated ADR (c) CCHP system with an integrated ADR and biogas upgrading unit (PWS/PSA).

The Conventional CCHP system (Fig. 2a) consists of a natural gas-powered ICE-PGU, waste heat recovery unit (WHR), natural gas boiler, lithium-bromide absorption chiller, heating coils, and infrastructure which connects the system to the national electricity grid. The PGU is responsible for generating electricity to meet the building's electric load (E_{pgu}). If the electric load is greater than the PGU's capacity the surplus electricity required is purchased from the national grid (E_{grid}). Waste heat from the PGU (Q_{pgu}) is collected by the WHR where it is then used to satisfy the buildings thermal load (Q_{whr}). The thermal load of all the CCHP systems in this study includes both the building's heating load (Q_h), distributed by heating coils (Q_{hc}), and the building's cooling load (Q_c) provided via a thermally activated absorption chiller (Q_{ac}). If the thermal load fails to be met by the WHR alone then the natural gas auxiliary boiler unit will be used to make up the remainder (Q_b). The PGU used in this study is the internal combustion engine (ICE). The Lithium-Bromide Absorption Chillers were the most compatible with ICEs, had relatively low investment costs, a high COP, non-toxic/inflammable working fluids, and low working costs, thus making them the favorable choice over other thermal activated cooling units for integration into the CCHPs optimized in this study.

Fig. 2(b) presents the energy flow of CCHP system with an integrated ADR. This system works on the same principle as the conventional CCHP system, however an integrated ADR, fed with a cattle manure feedstock, produces enough biogas to supply a biogas-compatible ICE operating at maximum load, 24-hours a day, 7-days a week (so long as it is provided

with feedstock). Any biogas not utilized by the PGU is sent to the stack to be exhausted into the atmosphere.

CCHP System with an integrated ADR and PWS unit is presented in Fig. 2 (c). This system works by the same principle as the conventional CCHP system differs from the ADR-CCHP since it has a pressurized water scrubbing (PWS) unit. The unit cleans the biogas before injection into the PGU to a composition of 97% methane (biomethane) which is of high enough quality to be injected into the national gas grid. As a result, a standard ICE can accept the biomethane and is therefore used in this system. Additionally, any excess gas not used by the CCHP can be sold to the national grid; as long as the infrastructure is available.

CCHP System with an integrated ADR and pressure swing absorption unit (PSA) is also presented in Fig. 2 (c). Pressure Swing Absorption (PSA) and Pressurized Water Scrubbing (PWS) are biogas upgrading technologies which have the lowest initial investment costs, have greater versatility, and do not require additional compression if the produced gas were to be fed into the national grid. It is the most mature technology of its kind [28,29]. Therefore, it is these two technologies which will be trialed and tested in the configurations of the CCHPs optimized in this study.

In the models that make use of FEL, the CCHP system prioritize satisfaction of the respective building's electric load and for any electricity demand more than the PGU's capacity, the deficiency is covered by the national grid. The exhaust heat from the PGU is considered the by-product and is gathered by the WHR unit before being utilized to meet as much of the thermal load as possible. The thermal deficiency is covered by the natural gas boiler unit. The models that use FTL sees the CCHP system prioritize meeting the

demand of the thermal load and any thermal demand more than the CCHP's output ability (constrained by equipment capacities and efficiencies) is covered by the natural gas boiler unit. The electricity generated by the PGU is considered the by-product and is utilized to meet as much of the building's electric load as possible. If there is an electric deficiency it is covered by the national grid. If the electrical by-product generated by the PGU is more than required, the surplus electricity can be sold to the grid so long as the infrastructure is in place in the location where the CCHP system is being utilized.

The mathematical model for the systems is described using Equations 8-50. The values of the technical parameters in these equations have been presented in Table 2.

The Parasitic Electricity Consumption of the Biogas Upgrading Systems, E_{pws}/E_{psa} (kWh), makes use of the same equations for both FEL and FTL systems:

$$E_{pws} = PWS_{max} \left(0.3 + \left((400 - PWS_{max}) \left(\frac{0.07}{1600} \right) \right) \right) \quad (8a)$$

$$E_{psa} = PSA_{max} \left(0.3 + \left((400 - PSA_{max}) \left(\frac{0.1}{1600} \right) \right) \right) \quad (8b)$$

In the equations above [28], PWS_{max} and PSA_{max} are the operational capacities of the PWS (kWh) and PSA (kWh).

The total Electricity Consumption of the System, E_{total} (kWh) is described for (a) ADR, (b) PWS and (c) PSA:

$$E_{total} = E + E_{ad} \quad (9a)$$

$$E_{total} = E + E_{ad} + E_{pws} \quad (9b)$$

$$E_{total} = E + E_{ad} + E_{psa} \quad (9c)$$

E is the electrical load of the building (kWh), and E_{ad} is the parasitic electrical consumption of the ADR (kWh) (assumed to be a fixed value, independent of the ADR's capacity) [30].

Electrical Indexing Matrix A (used to determine the Grid-PGU electrical output ratio) is

applicable for FEL systems only:

$$A = E_{total} \leq PGU_{max} \quad (10)$$

Electrical Indexing Matrix B (used to determine the Grid-PGU electrical output ratio), is

applicable for FEL systems only:

$$B = E_{total} > PGU_{max} \quad (11)$$

PGU_{max} is the electrical output capacity of the PGU (kWh).

The electrical output of the PGU, when acting as the sole source of power meaning no grid electricity is used, E_{pgu1} (kWh) is only applicable to FEL systems:

$$E_{pgu1} = A * E_{total} \quad (12)$$

E_{grid} (kWh) is the electrical output of the grid for (a) FEL and (b) FTL systems:

$$E_{grid} = E_{total} - PGU_{max} \quad (13a)$$

$$E_{grid} = E_{total} - E_{pgu} \quad (13b)$$

The Electrical output of the PGU when used concurrently with grid electricity, E_{pgu2} (kWh) is applicable to FEL systems only:

$$E_{pgu2} = (B * E_{total}) - E_{grid} = PGU_{max} \quad (14)$$

Total electrical output of PGU, E_{pgu} (kWh) is described by the equations below,

$$E_{pgu} = E_{pgu1} + E_{pgu2} \quad (15a)$$

$$E_{pgu} = F_{pgu} * \eta_{pgu} \quad (15b)$$

where η_{pgu} is the electrical efficiency of the PGU.

Excess electricity to be sold to the grid, E_{ex} (kWh) is only applicable to FTL systems:

$$E_{ex} = E_{pgu} - E_{total} \quad (16)$$

The total fuel consumption of PGU, F_{pgu} (kWh), is shown for (a) FEL systems and (b) FTL systems:

$$F_{pgu} = \frac{E_{pgu}}{\eta_{pgu}} \quad (17a)$$

$$F_{pgu} = \frac{QR_{whr}}{\eta_{whr} * (1 - \eta_{pgu})} \quad (17b)$$

In these equations η_{whr} is the thermal efficiency of the WHR unit, and QR_{whr} is the total exhausted heat recovered by the WHR (kWh).

The Volumetric Capacity of ADR, AD_{max} (m³), is shown for (a) ADR and (b) PWS and PSA systems,

$$AD_{max} = \frac{PGU_{max}}{EP_{ad} * \eta_{pgu}} \quad (18a)$$

$$AD_{max} = \frac{PGU_{max}}{EP_{adu} * \eta_{pgu}} \quad (18b)$$

where EP_{ad} is the electrical potential of the ADR (kWh/m³) and EP_{adu} is the electrical potential of the ADR when in tandem with a PWS/PSA (kWh/m³).

The Operational Capacity of PWS/PSA, PWS_{max}/PSA_{max} (m³/h), is described for (a) PWS and (b) PSA:

$$PWS_{max} = \frac{PGU_{max}}{EC_{ub} * \eta_{pgu}} \quad (19a)$$

$$PSA_{max} = \frac{PGU_{max}}{EC_{ub} * \eta_{pgu}} \quad (19b)$$

In these equations EC_{ub} is the energy content of upgraded biogas (Biomethane) with 97% CH₄ (kWh/m³).

The thermal energy required to meet building's heating load, Q_{req_hb} (kWh) is described by,

$$Q_{req_hb} = \frac{Q_h}{\eta_{he}} \quad (20)$$

where Q_h is the building's heating load (kWh), and η_{he} is the thermal efficiency of the heat exchanger.

Q_{req_ad} (kWh) is the thermal energy required to meet ADR's heating load:

$$Q_{req_ad} = \frac{AD_{max} * H_{ad}}{\eta_{he}} \quad (21)$$

In the equation above H_{ad} is the hourly thermal energy consumption factor of the ADR (kWh/h).

The thermal energy required to meet absorption chiller's cooling load, Q_{req_c} (kWh) is.

$$Q_{req_c} = \frac{Q_c}{COP_{ac}} \quad (22)$$

Q_c is the building's cooling load (kWh), and COP_{ac} is the coefficient of performance of the absorption chiller.

Q_{req_h} (kWh) is the total thermal energy required to satisfy the heating load of the building and ADR and is only applicable to FEL systems.

$$Q_{req_h} = Q_{req_hb} + Q_{req_ad} \quad (23)$$

The total thermal energy required to be provided by the system, Q_{totreq} (kWh), is only applicable to FTL systems:

$$Q_{totreq} = Q_{req_c} + Q_{req_ad} + Q_{req_hb} \quad (24)$$

Maximum fuel consumption of PGU, F_{pgumax} (kWh) is only applicable to FTL systems:

$$F_{pgumax} = \frac{PGU_{max}}{\eta_{pgu}} \quad (25)$$

Maximum thermal energy potentially recovered by WHR, Q_{whrmax} (kWh), is only applicable to FTL systems.

$$Q_{whrmax} = F_{pgumax} * (\eta_{whr}(1 - \eta_{pgu})) \quad (26)$$

Thermal energy indexing matrix A (used to determine the WHR-Boiler thermal output ratio), that is applicable to FTL systems is described by:

$$A = Q_{totreq} \leq Q_{whrmax} \quad (27)$$

Thermal output of the WHR when acting as the sole source of heat (no boiler heat used), Q_{whr1} (kWh), the is applicable to FTL systems is calculated as follow:

$$Q_{whr1} = A * Q_{totreq} \quad (28)$$

The thermal output of the boiler, Q_b (kWh), is described for (a) FEL systems and (b) FTL systems,

$$Q_b = Q_{b_ac} - Q_{b_h} \quad (29a)$$

$$Q_b = Q_{totreq} - Q_{whrmax} \quad (29b)$$

where Q_{b_ac} and Q_{b_h} are the thermal output of the auxiliary boiler used to meet the building's outstanding cooling load (kWh) and heating load (kWh) respectively.

Q_{whr2} (kWh) is the thermal output of WHR when used concurrently with the auxiliary boiler.

This is only applicable to FTL systems:

$$Q_{whr2} = (B * Q_{totreq}) - Q_b \quad (30)$$

The total thermal output of WHR, Q_{whr} (kWh), for (a) FEL systems and (b) FTL systems:

$$Q_{whr} = F_{pgu} * (\eta_{whr}(1 - \eta_{pgu})) \quad (31a)$$

$$Q_{whr} = Q_{whr1} + Q_{whr2} \quad (31b)$$

Q_{he} (kWh) is the thermal output of building's heat exchanger (heating coil) for (a) FEL systems and (b) FTL systems,

$$Q_{he} = (Q_{whr} + Q_{bgb_h} + Q_{b_h}) * \eta_{he} \quad (32a)$$

$$Q_{he} = (Q_{whr} + Q_b) * \eta_{he} \quad (32b)$$

where Q_{bgb_h} is the total heat output of biogas boiler used to meet heating load (kWh).

The fuel consumption of auxiliary boiler, F_b (kWh), is calculated using:

$$F_b = \frac{Q_b}{\eta_b} \quad (33)$$

F_{grid} (kWh) is the fuel consumption of grid to produce outstanding electric load:

$$F_{grid} = \frac{E_{grid}}{\eta_{grid} * \eta_{e_{css}}} \quad (34)$$

In this equation η_{grid} is the grid transmission efficiency and $\eta_{e_{css}}$ is the electrical efficiency of the CSS.

The total fuel consumption of the CCHP system, F_{cchp} (kWh) is described by:

$$F_{cchp} = F_{grid} + F_b + F_{pgu} \quad (35)$$

The total heating load not satisfied using thermal energy from WHR, Q_{rem_h} (kWh), is applicable to FEL systems only.

$$Q_{rem_h} = Q_{req_h} - Q_{whr} \quad (36)$$

Recovered heat available to be used by absorption chiller, $Q_{whr_ac_avl}$ (kWh), is applicable to FEL systems:

$$Q_{whr_ac_avl} = Q_{whr} - Q_{req_h} \quad (37)$$

The total unused (exhausted) recovered heat, Q_{whr_ex} (kWh),

$$Q_{whr_ex} = Q_{whr_ac_avl} - Q_{whr_ac} \quad (38)$$

where Q_{whr_ac} is the total WHR input into the absorption chiller (kWh).

The Annual biogas yield, BG_{yield} (m³) is determined using the following equation:

$$BG_{yield} = AD_{max} * 8760 \quad (39)$$

AD_{ex} (m³) is the ADR biogas yield not used by PGU (excess), for (a) ADR and (b) PWS and PSA systems:

$$AD_{ex} = \frac{AD_{max} - F_{pgu}}{EP_{ad}} \quad (40a)$$

$$AD_{ex} = \frac{AD_{max} - F_{pgu}}{EP_{adu}} \quad (40b)$$

The heat energy available from excess biogas yield, SBG_{avl} (kWh), for (a) ADR and (b) PWS and PSA systems:

$$SBG_{avl} = AD_{ex} * EP_{ad} \quad (41a)$$

$$SBG_{avl} = AD_{ex} * EP_{adu} \quad (41b)$$

Q_{bgb_ac} (kWh) is the thermal output of biogas boiler to meet building's cooling load for FEL systems:

$$Q_{bgb_ac} = SBG_{avl} \quad (42)$$

*Capped at Q_{req_c}

The thermal output of biogas boiler to meet the heating load, Q_{bgb_h} (kWh) for FEL systems:

$$Q_{bgb_h} = SBG_{avl} - Q_{bgb_{ac}} \quad (43)$$

*Capped at Q_{req_h}

The total thermal output of biogas boiler, Q_{bgb} (kWh), applicable to FEL systems is determined using:

$$Q_{bgb} = Q_{bgb_h} + Q_{bgb_{ac}} \quad (44)$$

SBG_{used} (m^3) is the excess biogas used by biogas boiler for (a) ADR and (b) PWS/PSA systems. This is only applicable to FEL systems.

$$SBG_{used} = \frac{Q_{bgb}}{EP_{ad}} \quad (45a)$$

$$SBG_{used} = \frac{Q_{bgb}}{EP_{adu}} \quad (45b)$$

The excess biogas after biogas boiler use, SBG_{ex} (m^3), that is applicable for FEL systems is described by:

$$SBG_{ex} = AD_{ex} - SBG_{used} \quad (46)$$

The Utilisation Factor of ADR biogas yield, BG_{uf} (%), applicable for FEL systems:

$$BG_{uf} = 1 - \left(\frac{SBG_{ex}}{BG_{yield}} \right) * 100 \quad (47)$$

Heat load remaining to be satisfied after surplus ADR biogas yield is used, $Q_{rem_{h2}}$ (kWh) for FEL systems:

$$Q_{rem_{h2}} = Q_{rem_h} - Q_{bgb_h} \quad (48)$$

The thermal output of auxiliary boiler used to meet outstanding heating load (not satisfied by biogas boiler), Q_{b_h} (kWh), that is applicable to FEL systems:

$$Q_{b_h} = Q_{rem_{h2}} \quad (49)$$

The Primary Energy Consumption (PEC) of the CCHP system, PEC_{cchp} (kWh) is calculated using the following equation:

$$PEC_{cchp} = \sum F_{cchp} \quad (50)$$

2.3. Particle Swarm Optimization Algorithm

The optimization method using in this study is the Particle Swarm Optimization Algorithm (PSOA). PSOA was first proposed by Eberhart and Kennedy in 1995 and was developed based upon the metaphor of the social behavior of migrating animals (such as insects, birds and fish). The principle of PSOA is that there are several, initially, randomly distributed “particles” (discrete solution points within the design space) which form a “swarm” situated within a search space. The search space is the set of all possible solutions to the respective optimization problem. Each particle within the swarm represents a candidate solution to the optimization problem and can be denoted by a position vector (x_i^k) and velocity vector (v_i^k) within the search space. During the coding of the algorithm the user specifies a lower and upper limit of the search space and defines the number of iterations to be executed. After each iteration of the optimization algorithm the particles that form the swarm move around in the search space, however this movement is not one of an arbitrary nature and is in fact a calculated decision determined via communication with the rest of the particles within the swarm.

Each particle has a memory of its own best position within the search space ($Pbest_i^k$). Between each iteration, the particles communicate with one another, updating the entire swarm on what the best position they have currently found within the search space is. By collaborating to share this knowledge, the swarm can then identify the global best position ($gbest^k$) in the search space. Using knowledge of their own $Pbest_i^k$ and the swarm’s $gbest^k$, the particles then execute a calculated movement, improving their positions within

the search space in a direction somewhere between the two. This cycle repeats with the particle's $Pbest_i^k$ and the swarm's $gbest^k$ values constantly being updated and communicated within the swarm between each iteration. Eventually all particles will have moved to the same point in the search space which will be the optimum location with respect to the specified objective function.

2.3.1. Criterion Equations and Decision Variables

The decision variable is the input variable to the objective function of the PSOA and is what is metaphorically the “particle position”. The decision variable's value will be adjusted by the PSOA until the value which optimises the objective function is identified. Since the CCHP subsystems' installed capacity mainly depends on the designed PGU's installed capacity, in this study, it is assumed that the installed capacity of the PGU (PGU_{max}) is the only decision variable. Once the optimum PGU capacity is calculated, the CCHP subsystem's optimum capacities are calculated accordingly.

The criterion equations are part for the objective of this study. These are described in Equations 51-60. The values of the technical parameters in these equations have been presented in Table 2.

The Overall Performance Index (OPI) of the CCHP systems (%) is described by:

$$OPI = PESR + ATCSR + CERR \quad (51)$$

In the equation PESR is the primary energy saving ratio, ATCSR is the annual total cost savings ratio and CERR is the carbon emissions reduction ratio.

The Primary Energy Savings Ratio (PESR) between the CCHP systems and the CSS (%) is determined by:

$$PESR = \left(\frac{PEC_{CSS} - PEC_{ADR-CCHP}}{PEC_{CSS}} \right) * 100 \quad (52)$$

The Annual Total Cost Savings Ratio (ATCSR) between the CCHP systems and the CSS (%) is calculated using Equation 54:

$$ATCSR = \left(\frac{ATC_{CSS} - ATC_{ADR-CCHP}}{ATC_{CSS}} \right) * 100 \quad (53)$$

The Annual Total Costs (ATC) of a corresponding energy system (€) is calculated using Equations 55-58:

$$ATC = (AEC + AEQC + OMC) \quad (54)$$

The Annual Energy Costs (AEC) of a corresponding energy system (€) is,

$$AEC = \sum_1^{8760} (F_{pgu} * UP_{fuel}) + (F_b * UP_{ng}) + (F_{grid} * UP_{ge}) \quad (55)$$

where UP_{fuel} denotes the unit price of the respective fuel being used by the PGU (€/kWh), UP_{ng} is the unit price of natural gas (€/kWh), and UP_{ge} is the unit price of grid electricity (€/kWh).

The capital recovery factor, R (%) is calculated:

$$R = \frac{i(1+i)^n}{(1+i)^n - 1} \quad (56)$$

In this equation i is the interest rate, and n is the service life of the corresponding equipment (years). In this study, the service life of all equipment is assumed to be of an equal value of 15 years.

The Annual Equipment Capital Costs (AEQC) of a corresponding energy system (€) is,

$$AEQC = R * \left(\sum_{k=1}^l N_k C_k \right) \quad (57)$$

where N_k is the installed capacity of the k^{th} equipment (kWh), and C_k is the initial capital cost of the k^{th} equipment (€).

Finally, the Annual Operation and Maintenance Costs (OMC) of a corresponding energy system (€) is,

$$OMC = \sum_{k=1}^l N_k OMC_k \quad (58)$$

where OMC_k , is the annual operation and equipment costs per unit capacity of the k^{th} equipment (€/kWh).

The Carbon Emissions Reduction Ratio (CERR) between the CCHP systems and the CSS (%) is calculated using Equation 60:

$$CERR = \left(\frac{CE_{CSS} - CE_{ADR-CCHP}}{CE_{CSS}} \right) * 100 \quad (59)$$

The Annual Carbon Emissions (CE) of a corresponding energy system (kg) is,

$$CE = \sum_1^{8760} (F_{pgu} * CE_{fuel}) + (F_b * CE_{ng}) + (F_{grid} * CE_{ge}) \quad (60)$$

where CE_{fuel} is the carbon emissions per unit of fuel used by the PGU (kg/kWh), CE_{ng} is the carbon emissions per unit of natural gas (kg/kWh), and CE_{ge} is the carbon emissions per unit of grid electricity (kg/kWh).

2.3.2. Objective Function

A weighted for of the Overall Performance Index (OPI), Equation 51, will be used as the objective function in this study.

The objective function is the mathematical function being optimised by the PSOA and depending on the goal of the study will either be minimised or maximised. The objective function to be used in this study and **maximised** is the same as in most CCHP optimisation studies, as identified by the literature survey, and is as follows:

$$Obj_f = \omega_1 ATCSR + \omega_2 CERR + \omega_3 PESR \quad (61)$$

$\omega_1, \omega_2,$ and ω_3 are the respective weight coefficients of each of the criterion.

$$0 \leq \omega_1, \omega_2, \omega_3 \leq 1 \quad (62a)$$

$$\omega_1 + \omega_2 + \omega_3 = 1 \quad (62b)$$

Weight coefficients are assigned to the criterion to indicate their relevant importance to the optimisation solution. Since there is no agenda by which one criterion is favored over another, each will be weighted equally. Therefore:

$$\omega_1 = \omega_2 = \omega_3 = \frac{1}{3} \quad (63)$$

3. Results and discussions

Potential configurations of a CCHP system integrated with an ADR harnessing a cattle manure feedstock and biogas upgrading plant have been proposed, details of the modeling methodology have been explained. These six potential configurations are: ADR-CCHP (FEL); ADR-CCHP (FTL); PWS-CCHP (FEL); PWS-CCHP (FTL); PSA-CCHP (FEL) and PSA-CCHP (FTL). These six potential configurations and two conventional CCHP configurations - CCHP (FEL), CCHP (FTL) have been applied to a case study – an office building in a heating-dominated climate in the middle of European (Krakow, Poland).

At first, the optimum design configuration for each of the eight configurations with respect to Annual Total Cost Savings (ATCS), Carbon Emission Reduction (CER), and Primary Energy Consumption (PEC) has been derived. Results of a conventional separated system (typical energy system) applied to the case study are used as a benchmark for the objective function criterion for the optimization. Comparisons are made between these eight optimized configurations, six potential configurations, and two conventional CCHP systems. As a result, to substantiate whether such a system can be a feasible and beneficial technology used to satisfy energy loads within the European building sector.

3.1. Case Study in Krakow, Poland

The typical 9-story office building is built in a heating-dominated location in middle European (Krakow, Poland), with a usable floor area of 30,000 m² [31]. The building was awarded a gold mark in the Leadership in Energy and Environmental Design (LEED) certificate, demonstrating energy-saving and pro-ecological. It saves as much as 33% of energy compared to local standards; over 75% of the office building surface has access to daylight. The building demand for energy loads is presented in Fig. 3. The building heating and cooling loads required for the air conditioning are also estimated [32].

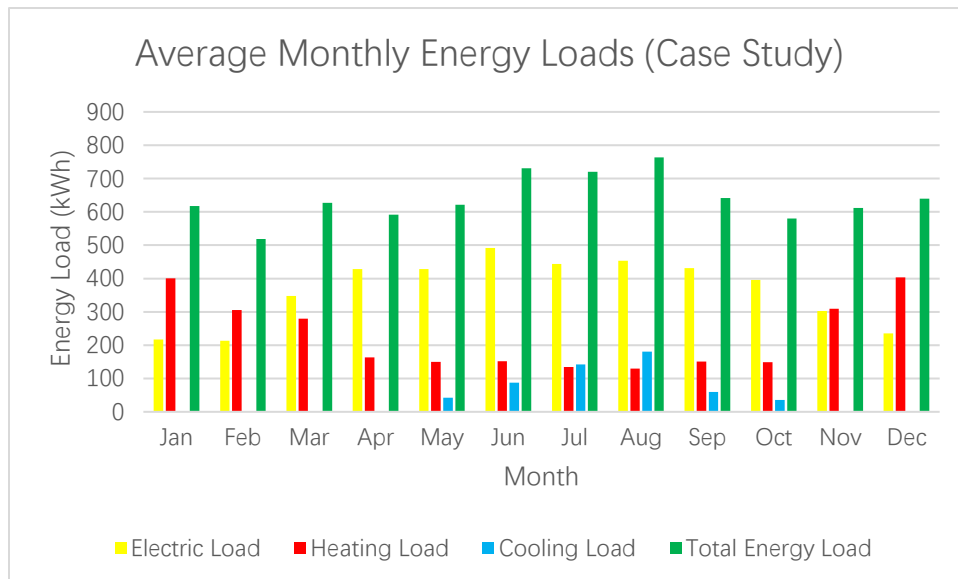


Fig. 3. Monthly energy demands of an office building in Krakow, Poland

3.2. Conventional separated system

Table 2 displays the technical parameters used for the CSS systems. Using the variables from Table 2, and applying them to Equations in Section 2.1, the CSS's benchmark values is calculated for each of the objective function's criterion (ATCSR, PESR, CERR) which

are to be optimized by the PSOA in section 2.3 for the eight configurations in Table 1.

Table 2: Parameters of the conventional separated system (reference)

| Parameter | Value | Unit | Reference |
|--|-------|--------|----------------------|
| Heat Exchanger (Heating Coil) Efficiency η_{he} | 75 | % | [5],[6],[13],[21] |
| Natural Gas Boiler System Efficiency η_b | 90 | % | - |
| Coefficient of Performance of Electric Chiller COP_{ec} | 3 | - | - |
| Electrical Efficiency of Conventional Separated System (CSS) η_{e_css} | 44 | % | [6] |
| Power Grid Electrical Transmission Efficiency η_{grid} | 83 | % | [6] |
| Carbon Emissions per Unit of Electricity from the Power Grid CE_{ge} | 0.256 | kg/kWh | [33] |
| Carbon Emissions per Unit of Natural Gas from the Gas Grid CE_{ng} | 0.184 | kg/kWh | - |
| Unit Price of Electricity from the Power Grid UP_{ge} | 0.122 | €/kWh | [34] |
| Unit Price of Natural Gas from the Gas Grid UP_{ng} | 0.039 | €/kWh | - |
| Service Life of Equipment (Assumed to be the Same for all Equipment in Each Design Configuration) SL | 15 | Years | [5],[6],[11],[20-22] |
| Interest Rate Applicable to Capital Costs IR | 5 | % | - |
| Capital Cost of Heating Coil CC_{hc} | 25 | €/kWh | - |
| Capital Cost of Natural Gas Boiler Unit CC_b | 45 | €/kWh | - |
| Capital Cost of Electric Chiller CC_{ec} | 110 | €/kWh | - |
| Operation and Maintenance to Capital Cost Ratio ϕ | 4 | % | - |
| Annual Operation & Maintenance Cost of Heating Coil OMC_{hc} | 1 | €/kWh | - |
| Annual Operation & Maintenance Cost of Natural Gas Boiler Unit OMC_b | 1.8 | €/kWh | - |
| Annual Operation & Maintenance Cost of Electric Chiller OMC_{ec} | 4.4 | €/kWh | - |

Table 3 - Conventional separated system Benchmarks for the Objective Function Criterion

| Month | TC (€) | CE (kg) | PEC (kWh) |
|-----------|---------|---------|-----------|
| January | 71,737 | 81,191 | 883,932 |
| February | 60,179 | 156,514 | 696,924 |
| March | 98,890 | 238,185 | 1,016,964 |
| April | 110,072 | 248,297 | 1,018,835 |
| May | 116,679 | 261,193 | 1,066,861 |
| June | 132,034 | 292,833 | 1,189,304 |
| July | 128,231 | 283,331 | 1,148,407 |
| August | 133,616 | 293,953 | 1,188,372 |
| September | 115,057 | 257,279 | 1,050,346 |
| October | 107,933 | 242,670 | 994,159 |
| November | 86,012 | 213,353 | 926,221 |
| December | 76,406 | 204,692 | 924,753 |

The CSS's benchmark values are shown in Table 3. It shows the primary energy consumption distribution and cost over a year with the highest energy consumption requirements during summer period. These values have been used to test performance of our multi-objective optimization approach and the objective function criterion. The set of optimal compromise solutions needs to be identified by an effective and complete search procedure to be able to carry out the best-case scenario. The six potential configurations: ADR-CCHP (FEL); ADR-CCHP (FTL); PWS-CCHP (FEL); PWS-CCHP (FTL); PSA-CCHP (FEL) and PSA-CCHP (FTL) and two conventional CCHP configurations - CCHP (FEL), CCHP (FTL) need to be optimized using the benchmark values as a reference point. The optimization is performed with the PSOA within the MATLAB environment. For the optimization of each configuration, results converge at less than 15 iterations, the simulation time is about 1.25 minutes.

3.3. Combined cooling, heating and power system

Tables 4, 5 and 6 display the technical parameters for eight configurations presented in Table 1. These technical parameters include values for energy, environment, and economics models for a combined cooling, heating, and power system. Applied with Equations in Section 2.2, they can be used for calculating the energy consumption, environmental impact, and economic cost of the CCHP systems. Table 4 includes the parameters used for calculations of PEC. These parameters include not only values for power generation but also those for waste heat recovery, heat exchanger and boiler efficiencies, power transmission efficiency, and energy consumption. Table 5 contains the environmental variables used for estimations of CER, such as carbon emissions per unit of fuel, carbon emissions per unit of electricity from the power grid, and gas grid. Table 6 presents economic variables utilized for calculations of ATCS, such as capital costs of equipment, operation, and maintenance costs, unit price of upgraded biogas, feed-in-tariff rate, service life of equipment, operation and maintenance to capital cost ratio, and annual operation & maintenance cost.

Table 4 - Parameters of the combined cooling, heating and power system – energy

| Parameter | Value | Units | Reference |
|---|--------|--------------------|-----------------------|
| Power generation unit electrical efficiency η_{pgu} | 38 | % | [33] |
| Waste heat recovery unit efficiency η_{whr} | 80 | % | [21] |
| Heat exchanger efficiency η_{he} | 75 | % | [5],[6], [13],[21] |
| Coefficient of performance of lithium bromide absorption chiller COP_{ac} | 0.72 | - | [13] |
| Natural gas auxiliary boiler efficiency η_b | 90 | % | [5],[6], [13],[21] |
| Power grid electrical transmission efficiency η_{grid} | 83 | % | [6] |
| Hourly electricity consumption of ADR E_{ad} | 1.51 | kWh | [30] |
| Hourly thermal energy consumption factor of ADR H_{ad} | 0.0678 | kWh/m ³ | - |
| Electrical potential of ADR EP_{ad} | 9.79 | kWh/m ³ | [36-38] |

| | | | |
|---|-------|--------------------|------|
| Electrical potential of ADR in tandem with PWS/PSA EP_{adu} | 16.32 | kWh/m ³ | - |
| Energy content of anaerobic digestion sourced biogas with 60% CH ₄ EC_{adb} | 5.8 | kWh/m ³ | [39] |
| Energy content of upgraded biogas (biomethane) with 97% CH ₄ EC_{ub} | 9.67 | kWh/m ³ | - |

Table 5: Parameters of the combined cooling, heating and power system – environment

| Parameter | Value | Units | Reference |
|--|-------|--------|-----------|
| Carbon Emissions per Unit of Electricity from the Power Grid CE_{ge} | 0.256 | kg/kWh | [34] |
| Carbon Emissions per Unit of Natural Gas from the Gas Grid CE_{ng} | 0.184 | kg/kWh | - |
| Carbon Emissions per Unit of Anaerobic Digestion Sourced Biogas with 60% CH ₄ CE_{adb} | 0 | kg/kWh | [40] |
| Carbon Emissions per Unit of Upgraded Biogas (Biomethane) with 97% CH ₄ CE_{ub} | 0 | kg/kWh | - |

Table 6: Parameters of the combined cooling, heating and power system – economic

| Parameter | Value | Unit | Reference |
|---|-------|-------|--------------------------|
| Unit Price of Electricity from the Power Grid UP_{ge} | 0.122 | €/kWh | [35] |
| Unit Price of Natural Gas from the Gas Grid UP_{ng} | 0.039 | €/kWh | - |
| Unit Price of Anaerobic Digestion Sourced Biogas with 60% CH ₄ UP_{adb} | 0.057 | €/kWh | [41] |
| Unit Price of Upgraded Biogas (Biomethane) with 97% CH ₄ UP_{ub} | 0.035 | €/kWh | - |
| Feed-in-Tariff Rate in Poland (for ADR's with a Capacity of 0 - 500kW) FIT | 0.127 | €/kWh | [42] |
| Feed-in-Premium Rate in Poland (for ADR's with a Capacity 500 - 1000kW) FIP | 0.146 | €/kWh | - |
| Service Life of Equipment (Assumed to be the Same for all Equipment in Each Design Configuration) SL | 15 | Years | [5],[6],[11], [20-22] |
| Interest Rate Applicable to Capital Costs IR | 5 | % | - |

| | | | |
|---|--------|------------------|------|
| Operation and Maintenance to Capital Cost Ratio ϕ | 4 | % | - |
| Operation & Maintenance Cost of Internal Combustion Engine (PGU) OMC_{pgu} | 44 | €/kWh | - |
| Operation & Maintenance Cost of Biogas Compatible Internal Combustion Engine (PGU) OMC_{bpgu} | 64 | €/kWh | - |
| Annual Operation & Maintenance Cost of Heating Coil OMC_{hc} | 1 | €/kWh | - |
| Annual Operation & Maintenance Cost of Natural Gas Boiler OMC_b | 1.8 | €/kWh | - |
| Annual Operation & Maintenance Cost of Biogas Boiler OMC_{bgb} | 2.62 | €/kWh | - |
| Annual Operation & Maintenance Cost of Waste Heat Recovery Unit OMC_{whr} | 3.2 | €/kWh | - |
| Annual Operation & Maintenance Cost of Lithium Bromide Absorption Chiller OMC_{ac} | 5.4 | €/kWh | - |
| Annual Operation & Maintenance Cost of Anaerobic Digestion Plant OMC_{ad} | 1,293 | €/m ³ | - |
| Annual Operation & Maintenance Cost of Pressurised Water Scrubber OMC_{pws} | 1453 | €/m ³ | - |
| Annual Operation & Maintenance Cost of Pressure Swing Absorption Unit OMC_{psa} | 1,360 | €/m ³ | - |
| Capital Cost of Internal Combustion Engine (PGU) CC_{pgu} | 1100 | €/kWh | - |
| Capital Cost of Biogas Compatible Internal Combustion Engine (PGU) CC_{bpgu} | 1600 | €/kWh | - |
| Capital Cost of Heating Coil CC_{hc} | 25 | €/kWh | - |
| Capital Cost of Natural Gas Boiler CC_b | 45 | €/kWh | - |
| Capital Cost of Biogas Boiler CC_{bgb} | 65 | €/kWh | - |
| Capital Cost of Waste Heat Recovery Unit CC_{whr} | 80 | €/kWh | - |
| Capital Cost of Lithium Bromide Absorption Chiller CC_{ac} | 135 | €/kWh | - |
| Capital Cost of Anaerobic Digestion Plant CC_{ad} | 11,533 | €/m ³ | [41] |
| Capital Cost of Pressurised Water Scrubber CC_{pws} | 11773 | €/m ³ | - |
| Capital Cost of Pressure Swing Absorption Unit CC_{psa} | 11,993 | €/m ³ | - |

For each of the eight CCHP configurations, using the ATCS, CER and PEC calculated

using parameters from Tables 4-6, the optimum installed capacity for each sub-system in each CCHP configuration is calculated and presented in Table 7.

Table 7 – Optimum design configuration for the eight CCHP systems

| System Configuration | AC_{max} (kWh) | AD_{max} (m^3) | B_{max} (kW h) | BGB $_{max}$ (kWh) | HC_{max} (kW h) | HE_{max} (kW h) | PGU $_{max}$ (kWh) | PSA $_{max}$ (m^3/h) | PWS $_{max}$ (m^3/h) | WHR $_{max}$ (kWh) |
|---|---------------------|-------------------------|---------------------|--------------------------|----------------------|----------------------|--------------------------|--------------------------------|--------------------------------|--------------------------|
| Conventional Separated System (Reference) | / | / | 727 | / | 545 | / | / | / | / | / |
| Conventional CCHP (FEL) | 244 | / | 338 | / | 545 | / | 438 | / | / | 572 |
| Conventional CCHP (FTL) | 244 | / | 291 | / | 545 | / | 343 | / | / | 436 |
| ADR-CCHP (FEL) | 244 | 111 | 75 | 336 | 545 | 8 | 413 | / | / | 539 |
| ADR-CCHP (FTL) | 244 | 86 | 315 | / | 545 | 6 | 321 | / | / | 419 |
| PWS-CCHP (FEL) | 244 | 62 | 299 | / | 545 | 4 | 383 | / | 104 | 500 |
| PWS-CCHP (FTL) | 244 | 47 | 350 | / | 545 | 3 | 292 | / | 79 | 381 |
| PSA-CCHP (FEL) | 244 | 62 | 297 | / | 545 | 4 | 387 | 105 | / | 505 |
| PSA-CCHP (FTL) | 244 | 47 | 348 | / | 545 | 3 | 293 | 80 | / | 382 |

3.3.1. Biogas/biomethane utilization factor

The proposed CCHP configurations integrated with an ADR harnessing a cattle manure feedstock and biogas upgrading plant produces excess biomethane; how to increase the utilization factor (UF) for optimization the system performance? There is no infrastructure in Poland for injecting any excess biomethane into the national gas grid. Thus, for ADR-CCHP's configuration, it is suggested to include a biogas compatible gas (BGB) boiler in the system for utilizing the excess biogas; for PWS-CCHP and PSA-CCHP, it is suggested to include a natural gas boiler (NGB). Table 8 presents the results of biogas/biomethane UF, with or without the boiler. Table 8 shows that for any of the systems utilizing the FTL operational strategy: ADR-CCHP System (FTL), PWS-CCHP System (FTL) and PSA-CCHP System (FTL), installation of boiler will not impact on the biogas/biomethane UF.

Table 8 – Adding biogas compatible or natural gas boiler to improve utilization factor

| System Configuration | Annual Biogas Yield (m ³) | Excess Biogas (m ³) | Excess Biomethane (m ³) | Utilisation Factor (%) |
|------------------------------|---------------------------------------|---------------------------------|-------------------------------------|------------------------|
| ADR-CCHP System (FEL) | 972,496 | 204,335 | / | 79.0 |
| ADR-CCHP System w/ BGB (FEL) | 972,496 | 157,009 | / | 83.9 ↑ |
| ADR-CCHP System (FTL) | 755,863 | 156,192 | / | 79.3 |
| ADR-CCHP System w/ BGB (FTL) | 755,863 | 156,192 | / | 79.3 - |
| PWS-CCHP System (FEL) | 541,002 | / | 70,178 | 87.0 |
| PWS-CCHP System w/ NGB (FEL) | 541,002 | / | 52,635 | 90.3 ↑ |
| PWS-CCHP System (FTL) | 412,461 | / | 69,757 | 83.1 |
| PWS-CCHP System w/ NGB (FTL) | 412,461 | / | 69,757 | 83.1 - |
| PSA-CCHP System (FEL) | 546,652 | / | 72,541 | 86.7 |
| PSA-CCHP System w/ NGB (FEL) | 546,652 | / | 54,816 | 90.0 ↑ |
| PSA-CCHP System (FTL) | 413,874 | / | 70,605 | 82.9 |
| PSA-CCHP System w/ NGB (FTL) | 413,874 | / | 70,605 | 82.9 - |

For any of the systems utilizing the FEL operational strategy: ADR-CCHP System (FEL), PWS-CCHP System (FEL) and PSA-CCHP System (FEL), with following observed results:

- ADR-CCHP:** UF increases by 4.9%, rising from 79.0% to 83.9%. This leads to a reduction in exhausted (waste) biogas of 47,326m³ per year. This is equivalent to 2.745GWh of energy being saved. This would also equate to a decrease in carbon emissions of 50,508kg per year.
- PWS-CCHP:** UF increases by 3.3% rising from 87.03% to 90.3%. This leads to a reduction in exhausted (waste) biomethane of 17,543m³ per year. This saves 1.696GWh

energy; it equates to reducing carbon emissions by 31,206kg for the year.

- **PSA-CCHP:** UF increases by 3.3% rising from 86.7% to 90.0%. This leads to a reduction in exhausted (waste) biomethane of 17,725 m³ per year. This is equivalent to 1.714GWh of energy being saved. It equates to a reduction in carbon emissions of 31,538kg for the year.

3.3.2. System performance evaluations

This study proposes six CCHP system configurations that integrate an ADR and biogas upgrading units such as PWS or PSA. The six CCHP systems are applied to a commercial office building to see whether they could technically and economically outperform an optimized conventional CCHP system. The objective function for the PSOA optimization is calculated using equally weighted results of ATCSR, CERR, and PESR. Fig. 4 presents the ATCSR for each CCHP configuration; Fig. 5 presents the CERR results for each configuration and Fig. 6 shows the PESR results. Fig. 7 compares the OPI of each system, explained in Section 2.3.1, OPI is a sum of the 3 criteria (CERR, PESR and ATCSR) to reflect the overall performance of each system.

In Fig. 4, the ATCSR of each CCHP configuration are calculated by comparing to cost of the CSS system, the higher ATCSR value shows the system saves more cost and is preferred. Almost all the eight configurations have positive ATCSR value, this demonstrates the CCHP systems can be a cheaper alternative for energy provision once energy loads are high enough to outweigh the higher capital costs incurred. The ATCSR increases when building energy demands increases.

Among the eight CCHP configurations, the conventional CCHP systems yielded much higher savings across the course of the year, with average of 53.9% deploying FTL, and

62.5% when deploying FEL. These equal to huge annual saving of €669,329 and €775,919, respectively. Compared to the CSS system, almost all the biogas CCHPs yielded an ATCSR of around 27%, which equals an average savings of approximately €335,000 for the year. Overall, the ATCSR of the conventional CCHP is approximate twice the values of the biogas CCHPs; the PSA-CCHP system that requires a biogas upgrading unit (PSA) has the lowest ATCSR value.

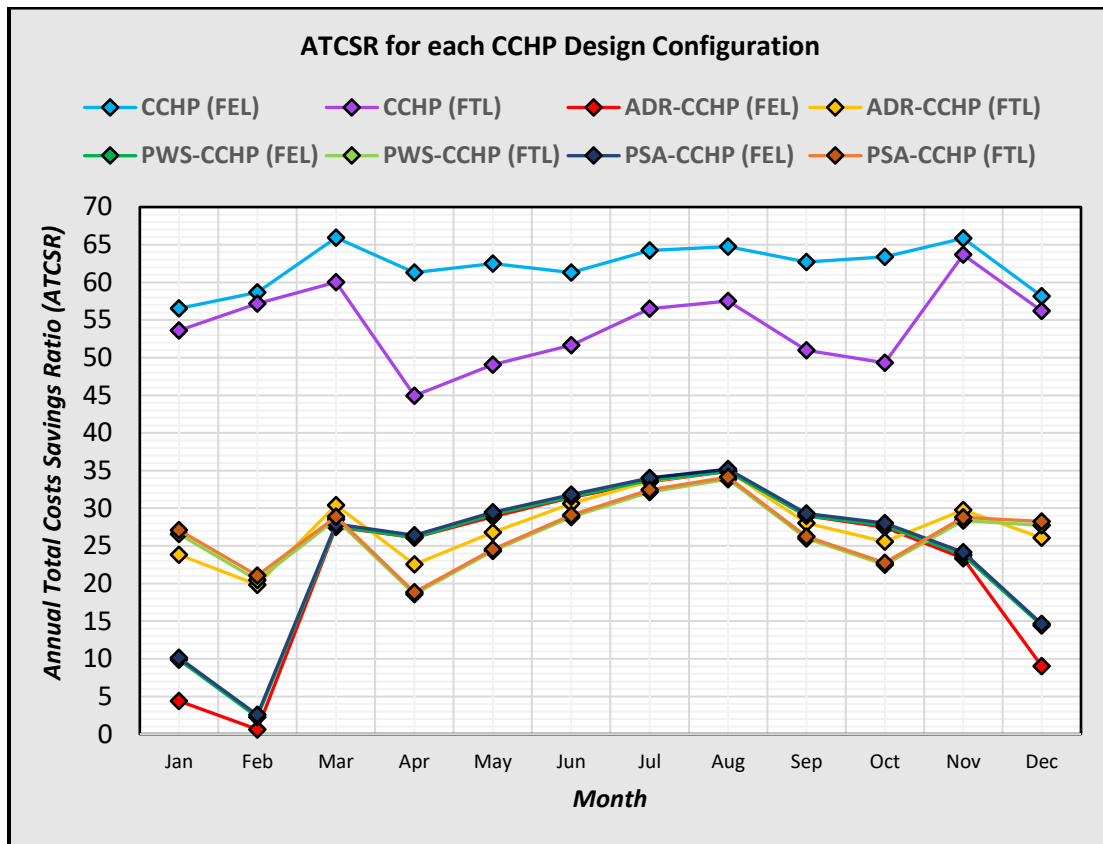


Fig. 4. Annual total cost saving ratio of the eight CCHP configurations

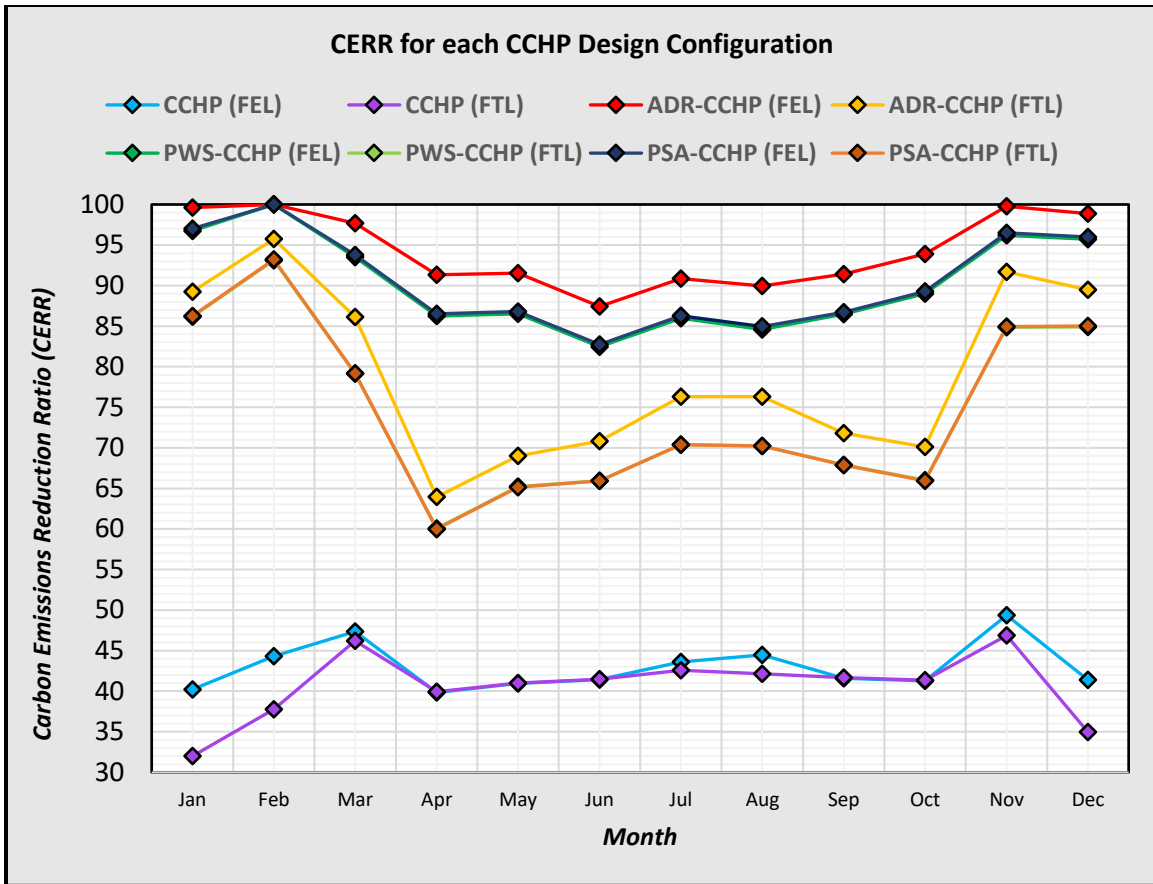


Fig. 5. Carbon emissions reduction ratio of the eight CCHP configurations

Fig. 5 presents the CERR of each CCHP configuration. The higher CERR value shows more carbon emission reductions of the CCHP system than the CSS system. All the CCHP configurations have positive CERR values, this shows that all eight systems are more environmentally friendly than the CSS system. The CERR decreases when the building energy demand increases from April to October. This is because the CCHPs become more dependent on sourcing electricity and gas from the grid, which present a much greater burden on the environment than the energy produced by the high-efficiency CCHP units, and especially those harnessing biogas/biomethane as their fuel source.

Unlike with the cost savings, the conventional CCHP systems fell short against the biogas CCHPs: averaging, between the two of them, a CERR of around 42%, which equals to

around 1.2 kt less carbon dioxide emissions into the atmosphere. The biogas CCHPs yielded carbon emission savings in the range of 73.1%, in the lowest case, up to an impressive 93.7% coming from the ADR-CCHP (FEL) with the integrated biogas boiler; an overall total carbon emission savings of 27.05 kt. In February, the ADR-CCHP and PSA-CCHP deploying FEL yielded a CERR of 100%, thus meaning that these systems produced zero carbon emissions during this month. The ADR-CCHP (FEL) also made zero carbon emissions in January and November and yielded a CERR of around 98% in December, equating to only 4094kg CO₂ for the entire month. For minimizing annual carbon emissions, the ADR-CCHP is the optimum solution.

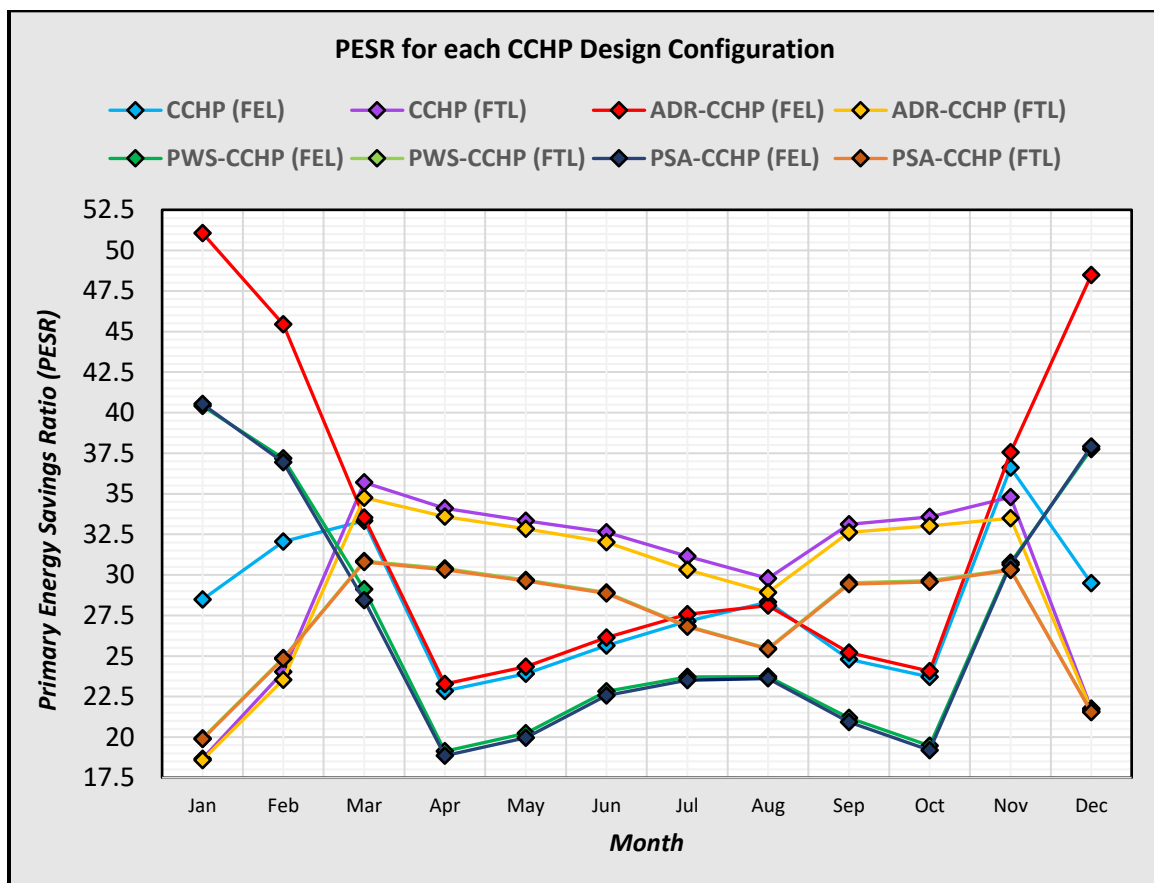


Fig. 6. Primary energy savings ratio of the eight CCHP configurations

Fig. 6 shows each of the CCHP systems operating under the FTL strategy presents their

worst PESR values in the winter months and best values in the summer months, whereas the CCHP systems deploying FEL show the contrary. This is because in the winter months, the thermal load exceeds the electrical load, benefitting the FEL strategy thus, less energy will be wasted using this method. Whereas the electrical load exceeds the thermal load in the summer months, the FTL operational strategy is the more energy-efficient option. The PESR value for each CCHP system was relatively close, with a variance of only 7.5% between the worst performer (PSA-CCHP, FEL) and the best performer (ADR-CCHP, FEL, with a BGB). The leads to an energy-saving of 8.59GWh/year. The best solution would be to prioritize the energy saving, the ADR-CCHP with an integrated BGB, deploying FEL.

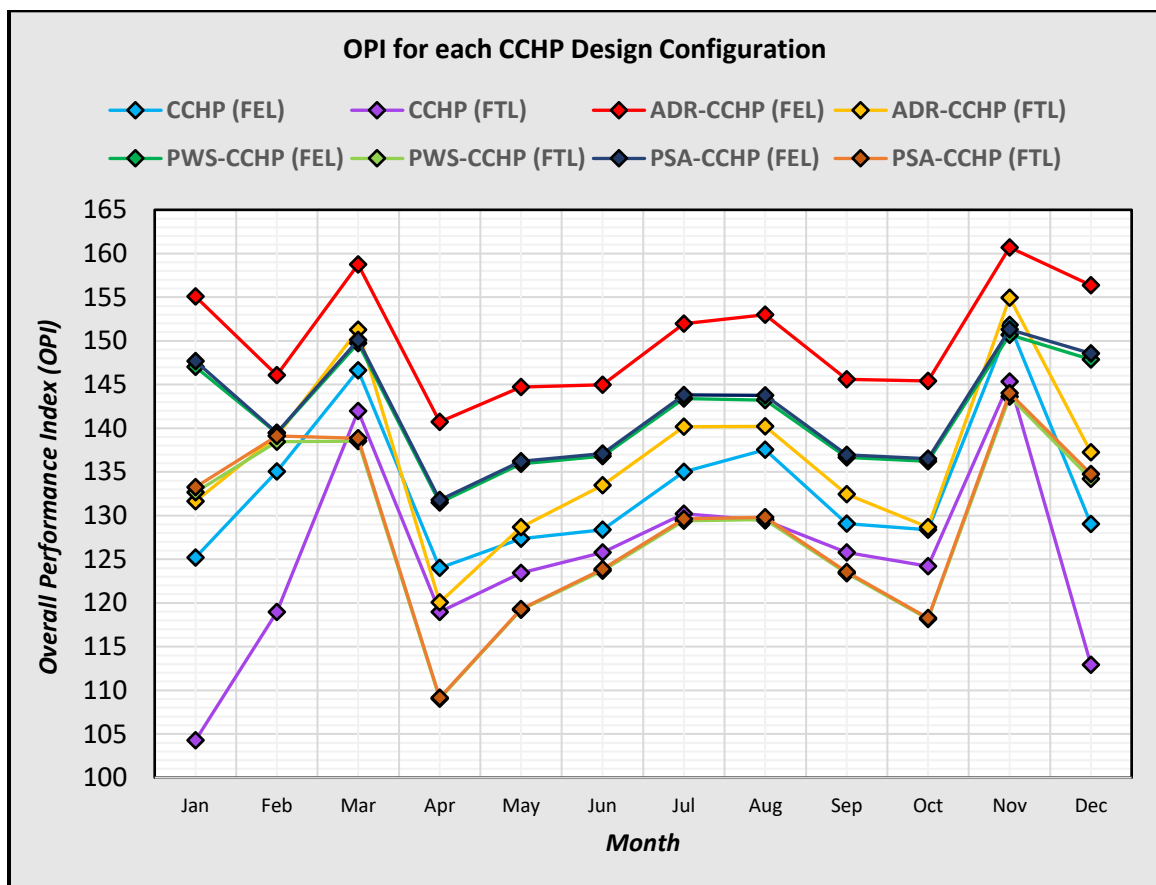


Fig. 7. Overall performance index of the eight CCHP configurations

Fig. 7 presents the OPI value, which is a sum of the CERR, PESR, and ATCSR to reflect

the overall performance of each system compared to a CSS system. Overall, the OPI value is higher in summer with higher building energy demand, and it decreases in winter when the energy demand decreases. All CCHP systems managed to yield an OPI value of more than 100%, meaning that in combined terms of Cost Savings, Carbon Emissions, and Energy Consumption, the eight CCHP systems all performed more than twice as well as the reference CSS system. The worst overall performing CCHPs were conventional CCHPs, which incorporated biogas upgrading plants deploying the FTL operational strategy. These 4 systems – CCHP (FEL), CCHP (FTL), ADR-CCHP (FTL), PSA-CCHP (FTL) scored an average OPI of around 130%. The best performing CCHP system, which performed 8.5% better than the second-best system, is the ADR-CCHP with an integrated BGB, deploying FEL. This CCHP system yielded an OPI of 151.14% and, as discussed above, is the best performing system in 2 of the 3 criteria optimized (CERR and PESR).

4. Conclusions

This paper proposes biogas fed CCHP systems that utilize and integrate an ADR harnessing a cattle manure feedstock with or without biogas upgrading technology. The systems are modeled and optimized to verify whether such configurations could be advantageous over CSSs and optimized conventional CCHP systems when applied in a case study. Using the PSO method, several optimized configurations of CCHP systems successfully achieve the aim. The results show that when considering the technical, economic, and environmental factors, the overall performance of all eight CCHP systems optimized in this research study proved to be significantly advantageous over the CSS system.

System configurations where CCHP is combined with either anaerobic digestion reactor (ADR), pressure swing absorption (PSA), or pressurized water scrubbing (PWS) showed

benefits over the optimized conventional gas fed CCHP systems, in terms of cost, CO₂ emissions, and primary energy consumption. The CCHP system with an integrated ADR, with a biogas boiler, deploying the following the electric load (FEL) operational strategy yields the best results. This system presents overall performance index (OPI) score of 151.1%, after achieving the best carbon emissions reduction (CER) score of 93.7%, and the best primary energy savings ratio (PESR) score of 32.0%.

Several subject areas could be further investigated to improve the ADR-CCHP system performance. This study identifies the optimum design configuration with cost, carbon emissions, and energy consumption - each of equal weight. Future research could consider employing the three weighting coefficients as objective functions variables to identify a different scenario in which a final user prefers one criterion over others. Current research focuses on optimizing the PGU's design, assuming the other CCHP subsystems' installed capability mainly depends on the PGU. Other CCHP subsystems are designed based on the optimized results of the PGU. Future work could investigate including other decision variables in the optimization process. Possibilities for future work could also be on feed in tariffs/premiums, thermal storage technologies, electrical storage technologies, hybridization with solar technologies, hybrid-chiller operational strategies, multiple power generation units, and different biomass feedstocks. The case study can be expanded to different climates, various building types for further understanding of the feasibility of the proposed system with integrated biofuel technologies.

Funding

This research did not receive any specific grant from funding agencies in the public, commercial, or not-for-profit sectors.

References

- [1] X. Cao, D. Xilei, J. Liu, Building energy-consumption status worldwide and the state-of-the-art technologies for zero-energy buildings during the past decade, *Energy and Buildings*, 128 (2016). <https://doi.org/10.1016/j.enbuild.2016.06.089>.
- [2] IEA, *Tracking Buildings*, (2020), IEA, Paris. <https://www.iea.org/reports/tracking-buildings-2020>.
- [3] IEA, *Global energy & CO2 status report (2019)*, IEA, Paris <https://www.iea.org/reports/global-energy-co2-status-report-2019>.
- [4] F.A. Al-Sulaiman, F. Hamdullahpur, I. Dincer, Trigeration: A comprehensive review based on prime movers, *International Journal of Energy Research*, 35 (2011) 233–258. <https://doi.org/10.1002/er.1687>.
- [5] J.J. Wang, Y.Y. Jing, C.-F. Zhang, Optimization of capacity and operation for CCHP system by genetic algorithm, *Applied Energy*. 87 (2010) 1325–1335. <https://doi.org/10.1016/j.apenergy.2009.08.005>.
- [6] D.E. Ghersi, M. Amoura, K. Loubar, U. Desideri, M. Tazerout, Multi-objective optimization of CCHP system with hybrid chiller under new electric load following operation strategy, *Energy*, 219 (2021). <https://doi.org/10.1016/j.energy.2020.119574>.
- [7] G. Yang, X. Zhai, Optimization and performance analysis of solar hybrid CCHP systems under different operation strategies, *Applied Thermal Engineering*. 133 (2018) 327–340. <https://doi.org/10.1016/j.applthermaleng.2018.01.046>.
- [8] Z. Zhao, B. Zou, The optimal operation strategy and simulation for CCHP system, *IOP Conf. Ser.: Earth Environ. Sci.* 168 (2018) 012007. <https://doi.org/10.1088/1755-1315/168/1/012007>.

- [9] J.J. Wang, T. Mao, J. Sui, H. Jin, Modelling and performance analysis of CCHP (combined cooling, heating and power) system based on co-firing of natural gas and biomass gasification gas, *Energy*. 93 (2015) 801–815. <https://doi.org/10.1016/j.energy.2015.09.091>.
- [10] X. Li, X. Kan, X. Sun, Y. Zhao, T. Ge, Y. Dai, C.-H. Wang, Performance analysis of a biomass gasification-based CCHP system integrated with variable-effect LiBr-H₂O absorption cooling and desiccant dehumidification, *Energy*. 176 (2019) 961–979. <https://doi.org/10.1016/j.energy.2019.04.040>.
- [11] J.J. Wang, Z.L. Xu, H.G. Jin, G. Shi, C. Fu, K. Yang, Design optimization and analysis of a biomass gasification based BCHP system: A case study in Harbin, China, *Renewable Energy*. 71 (2014) 572–583. <https://doi.org/10.1016/j.renene.2014.06.016>.
- [12] H. Ren, W. Zhou, K. Nakagami, W. Gao, Integrated design and evaluation of biomass energy system taking into consideration demand side characteristics, *Energy*. 35 (2010) 2210–2222. <https://doi.org/10.1016/j.energy.2010.02.007>.
- [13] D. Maraver, A. Sin, J. Royo, F. Sebastián, Assessment of CCHP systems based on biomass combustion for small-scale applications through a review of the technology and analysis of energy efficiency parameters, *Applied Energy*. 102 (2013) 1303–1313. <https://doi.org/10.1016/j.apenergy.2012.07.012>.
- [14] H. Cho, P.J. Mago, R. Luck, L.M. Chamra, Evaluation of CCHP systems performance based on operational cost, primary energy consumption, and carbon dioxide emission by utilizing an optimal operation scheme, *Applied Energy*. 86 (2009) 2540–2549. <https://doi.org/10.1016/j.apenergy.2009.04.012>.
- [15] A. Rong, R. Lahdelma, An efficient linear programming model and optimization

algorithm for trigeneration, *Applied Energy*. 82 (2005) 40–63.
<https://doi.org/10.1016/j.apenergy.2004.07.013>.

[16] B.K. Chen, C.C. Hong, Optimum operation for a back-pressure cogeneration system under time-of-use rates, *IEEE Transactions on Power Systems*. 11 (1996) 1074–1082.
<https://doi.org/10.1109/59.496197>.

[17] S. Ashok, R. Banerjee, Optimal operation of industrial cogeneration for load management, *IEEE Transactions on Power Systems*. 18 (2003) 931–937.
<https://doi.org/10.1109/TPWRS.2003.811169>.

[18] G. Chicco, P. Mancarella, Matrix modelling of small-scale trigeneration systems and application to operational optimization, *Energy*. 34 (2009) 261–273.
<https://doi.org/10.1016/j.energy.2008.09.011>.

[19] A.A. Rentizelas, I.P. Tatsiopoulos, A. Tolis, An optimization model for multi-biomass tri-generation energy supply, *Biomass and Bioenergy*. 33 (2009) 223–233.
<https://doi.org/10.1016/j.biombioe.2008.05.008>.

[20] H. Lin, C. Yang, X. Xu, A new optimization model of CCHP system based on genetic algorithm, *Sustainable Cities and Society*. 52 (2020) 101811.
<https://doi.org/10.1016/j.scs.2019.101811>.

[21] J. Wang, Z. (John) Zhai, Y. Jing, C. Zhang, Particle swarm optimization for redundant building cooling heating and power system, *Applied Energy*. 87 (2010) 3668–3679.
<https://doi.org/10.1016/j.apenergy.2010.06.021>.

[22] S.G. Tichi, M.M. Ardehali, M.E. Nazari, Examination of energy price policies in Iran for optimal configuration of CHP and CCHP systems based on particle swarm optimization algorithm, *Energy Policy*. 38 (2010) 6240–6250.

<https://doi.org/10.1016/j.enpol.2010.06.012>.

[23] A.D. Cuéllar, M.E. Webber, Cow power: the energy and emissions benefits of converting manure to biogas, *Environ. Res. Lett.* 3 (2008) 034002.

<https://doi.org/10.1088/1748-9326/3/3/034002>.

[24] EESI, E., Fact Sheet | Biogas: Converting Waste to Energy | White Papers | EESI. (2021). <https://www.eesi.org/papers/view/fact-sheet-biogasconverting-waste-to-energy>.

[25] W. Foster, U. Azimov P. Gauthier-Maradei, L. Castro Molano, M. Combrinck, J. Munoz, J. J. Esteves, L. Patino. Waste-to-energy conversion technologies in the UK: Processes and barriers – A review. *Renewable and Sustainable Energy Reviews* 2020; 135:110226.

[26] Truc T.Q. Vo, David M. Wall, Denis Ring, Karthik Rajendran, Jerry D. Murphy. Techno-economic analysis of biogas upgrading via amine scrubber, carbon capture and ex-situ methanation. *Applied Energy* 212 (2018) 1191–1202, <https://doi.org/10.1016/j.apenergy.2017.12.099>

[27] Veronika Vrbova and Karel Ciahotny. Upgrading Biogas to Biomethane Using Membrane Separation. *Energy Fuels* 2017, 31, 9393–9401, [10.1021/acs.energyfuels.7b00120](https://doi.org/10.1021/acs.energyfuels.7b00120)

[28] F. Bauer, C. Hulteberg, T. Persson, D. Tamm, Biogas upgrading - Review of commercial technologies, (2013), Sweden.

[29] I. Angelidaki, L. Treu, P. Tsapekos, G. Luo, S. Campanaro, H. Wenzel, P. Kougias, Biogas upgrading and utilization: Current status and perspectives, *Biotechnology Advances*. 36 (2018). <https://doi.org/10.1016/j.biotechadv.2018.01.011>.

[30] Y. Zhang, Anaerobic Digestion System - Energy Balance, (2013) 53.

http://www.valorgas.soton.ac.uk/Pub_docs/JyU%20SS%202013/VALORGAS_JyU_2013_Lecture%2013.pdf.

[31] J. Mikulik, Energy demand patterns in an office building: a case study in Kraków (Southern Poland), *Sustainability*. 10 (2018) 2901. <https://doi.org/10.3390/su10082901>.

[32] Energy Consumption Guide 19: Energy use in offices, United Kingdom, (2003).

[33] Campanari S, Macchi E. Technical and tariff scenarios effect on microturbine trigenerative applications. *Journal of Engineering for Gas Turbines and Power* 2004, 126(3), 581–589.

[34] Greenhouse gas reporting: conversion factors 2018, GOV.UK. (n.d.). <https://www.gov.uk/government/publications/greenhouse-gas-reporting-conversion-factors-2018> (accessed June 27, 2021).

[35] Poland electricity prices, September 2020, GlobalPetrolPrices.Com. (n.d.). https://www.globalpetrolprices.com/Poland/electricity_prices/ (accessed June 27, 2021).

[36] L. Rosenberg, G. Kornelius, Experimental investigation of biogas production from feedlot cattle manure, *Journal of Energy in Southern Africa*. 28 (2017). <https://doi.org/10.17159/2413-3051/2017/v28i4a1753>.

[37] L. Dong, G. Cao, X. Guo, T. Liu, J. Wu, N. Ren, Efficient biogas production from cattle manure in a plug flow reactor: A large-scale long-term study, *Bioresource Technology*. 278 (2019) 450–455. <https://doi.org/10.1016/j.biortech.2019.01.100>.

[38] H. Wang, H.A. Aguirre-Villegas, R.A. Larson, A. Alkan-Ozkaynak, Physical properties of dairy manure pre- and post-anaerobic digestion, *Applied Sciences* 9 (2019). 2703. <https://doi.org/10.3390/app9132703>.

[39] O. Eriksson, Environmental technology assessment of natural gas compared to biogas,

in: P. Potocnik , Natural Gas, Sciyo, 2010. <https://doi.org/10.5772/9837>.

[40] J.A. Medrano, M.A. Llosa-Tanco, V. Cechetto, D.A. Pacheco-Tanaka, F. Gallucci, Upgrading biogas with novel composite carbon molecular sieve (CCMS) membranes: Experimental and techno-economic assessment, Chemical Engineering Journal. 394 (2020) 124957. <https://doi.org/10.1016/j.cej.2020.124957>.

[41] Bernhard Sturmer, Franz Kirchmeyr, Kornel Kovacs, Frank Hofmann, David Collins, Claire Ingremeau, Jan Stambasky, Technical-economic analysis for determining the feasibility threshold for tradeable biomethane certificates, BIOSURF, 2016. <http://www.ergar.org/wp-content/uploads/2018/07/BIOSURF-D3.4.pdf>.

[42] Eclareon GmbH, Renewable energy policy database: tools list, (2012). <http://www.res-legal.eu/search-by-country/poland/tools-list/> (accessed June 17, 2021).